Title
Nitinol-based Nanotubular and Nanowell Coatings for the Modulation of Human Vascular Cell Functions

Author
Lee, Phin Peng

Publication Date
2015

Peer reviewed|Thesis/dissertation

Nitinol-based Nanotubular and Nanowell Coatings for the Modulation of Human Vascular Cell Functions

by

PHIN PENG LEE

DISSERTATION

Submitted in partial satisfaction of the requirements for the degree of

DOCTOR OF PHILOSOPHY

in

Bioengineering

in the

GRADUATE DIVISION

of the

UNIVERSITY OF CALIFORNIA, SAN FRANCISCO

AND

UNIVERSITY OF CALIFORNIA, BERKELEY

Dedicated to

miu

Abstract

Nitinol-based Nanotubular and Nanowell Coatings for the Modulation of Human Vascular Cell Functions

by

Phin Peng Lee

Doctor of Philosophy in Bioengineering

University of California, San Francisco

and

University of California, Berkeley

Current approaches to reducing restenosis do not balance the reduction of vascular smooth muscle cell proliferation with the increase in the healing of the endothelium. Here, I present my study on the synthesis and characterization of a nanotubular coating on Nitinol substrates. I found that the coating demonstrated 'pro-healing' properties by increasing primary human aortic endothelial cell spreading, migration and collagen and elastin production. Certain cellular functions such as collagen and elastin production were also found to be affected by changes in nanotube diameter. The coating also reduced the proliferation and mRNA expression of collagen I and MMP2 for primary human aortic smooth muscle cells. I will also demonstrate the synthesis of a nanowell coating on Nitinol stents as well as an additional poly(lactic-co-glycolic acid) coating on top of the nanowells that has the potential for controlling drug release. These findings demonstrate the potential for the coatings to aid in the prevention of restenosis and sets up future explorations of *ex vivo* and *in vivo* studies.

Contents

List of Figures

Chapter 1

Introductory Remarks

Heart disease places an enormous burden on America and is estimated to cost over $316 billion in the year 2010 alone, the majority of which is spent on coronary heart disease[1]. A substantial number of these patients who received percutaneous transluminal coronary angioplasty went on to suffer recurring ischemia. It has been reported that 30% to 60% of angioplasty patients suffer from restenosis within six months of the treatment[2]. Bare metal stents (BMS) helped in the prevention of early abrupt closure due to elastic recoil and generally improved patient outcomes but in-stent restenosis (ISR) rates were still reported to be around 20% to 30%[2–5].

ISR after BMS implantation has been mainly attributed to neointimal hyperplasia (NIH), which is the result of vascular smooth muscle cells (VSMC) responding to the injury caused during stenting[2–4,6]. These cells respond to the implantation by migrating into the vessel lumen, where they proliferate excessively and secrete an abundance of extra-cellular matrix (ECM) proteins, thereby re-narrowing the artery. The innovation of drug-eluting stents (DES) that release drugs that reduce the proliferation and migration of VSMC has successfully reduced ISR rates to below 10%[3]. However, the anti-proliferative drugs in DES are non-specific and affect endothelial cells (EC) as well, resulting in delayed healing and an increase in the rates of late stent thrombosis[7–11]. Specifically, drugs such as Paclitaxel and Rapamycin were known to increase the thrombogenic risk by reducing endothelial cell function, proliferation and migration[12,13].

Recent studies have shown that an upright nanotubular coating on titania substrates created via an anodization process has the potential to regulate EC and VSMC in a "pro-healing" manner[14,15]. When cultured on these nanotubes-coated substrates, VSMC have been shown to decrease in proliferation, motility and expression of genes related to inflammation, while EC have been shown to increase in proliferation, motility and secretion of prostaglandin I2 – an anti-thrombogenic and anti-proliferative agent for VSMC[14,15]. In light of these promising results, I have turned to synthesizing a nanotubular coating for a widely used material in FDA-approved biomedical devices – Nitinol[16]. Along with stainless steel and cobalt chromium, Nitinol is one of the three common materials used in stents[5]. However, its material properties offer distinct advantages – Nitinol-based stents have a variety of deployment methods while its superelasticity and kink-resistance also make it highly desirable for peripheral stents[16]. Here, I present an investigation on the effects of this coating on primary human aortic endothelial cells (HAEC) and human aortic smooth muscle cells (HASMC), with a focus on the potential for the prevention of restenosis.

Chapter 2

Synthesis and Characterization of Nanotubular Coating

Previously, Kim et al. presented a study on the synthesis of small-diameter (38nm) NiO – TiO_2 nanotubes as electrodes for supercapacitors[17]. Building on that for this study, I aimed to synthesize a nanotubular coating on Nitinol with controlled diameters through the variation of the anodization parameters such as voltage, duration and electrolyte concentration[17].

2.1 Synthesis of nanotubular coatings.

Nitinol foils were purchased from two sources (55.85 wt% Ni, light oxide surface, NDC, USA and 55.75 wt% Ni, superelastic, pickled surface, Alfa Aesar, USA). These were cut into 1 cm by 1 cm pieces and cleaned sequentially using an ultrasonicator with dilute micro-90 solution (International Products Corporation), acetone and ethanol. They were dried in nitrogen and placed in an anodization setup with the Nitinol foil as the working electrode and a platinum foil (Alfa Aesar, 0.1-mm-thick, 1.5 cm by 3 cm, 99.99%) as the counter electrode, 7 cm directly apart in a Teflon container (Figure 1).

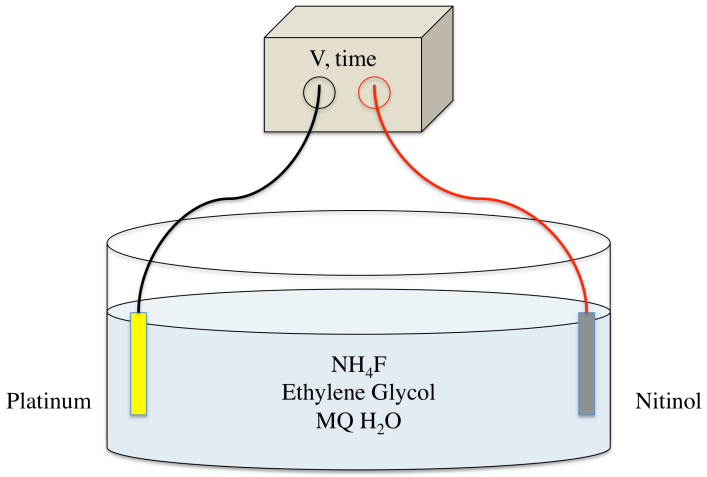

Figure 1. A schematic of the anodization setup used for the synthesis of the Nitinol-based nanotubular coating.

The optimum anodization conditions required to produce a nanotubular coating were obtained via a series of iterations beginning from 2 initial anodization conditions. The concentration of NH_4F in the electrolyte solution, voltage and/or duration of anodization were varied after each iteration based on the images examined under Scanning Electron Microscopy (Carl Zeiss Ultra 55 FE-SEM, San Francisco State University). Figure 2 shows several SEM images of the failed attempts.

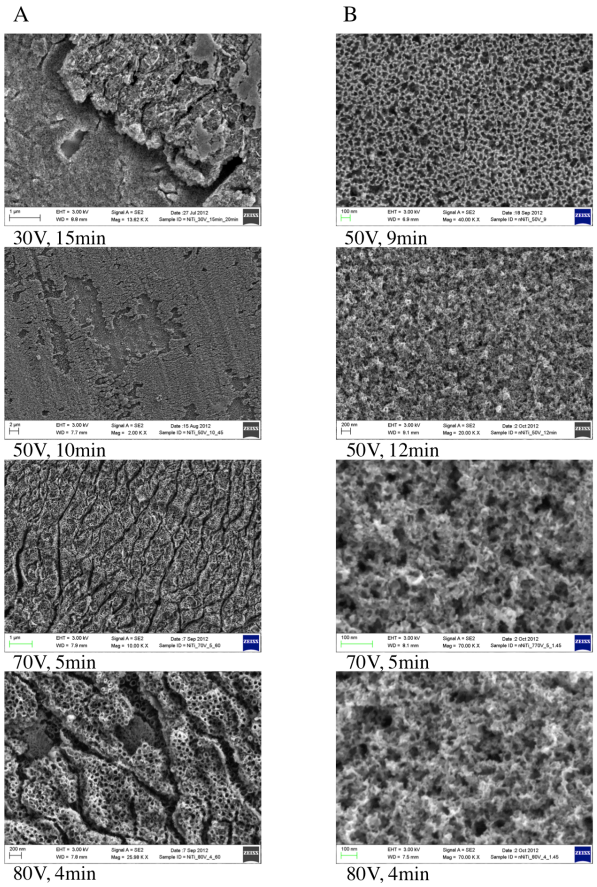

Figure 2. SEM images of several failed iterations of the anodization process.

Although I was unable to produce a homogenous, fully exposed nanotubular coating on the Nitinol foil purchased from NDC, I obtained a nanotubular coating on the Nitinol foils purchased from Alfa Aesar under the following conditions: the electrolyte solution consists of 1.48 g of NH_4F (Sigma-Aldrich), 490 mL of ethylene glycol (Sigma-Aldrich) and 8.35 mL of Millipore water; the anodization voltage and duration were 85 V and 4 minutes respectively.

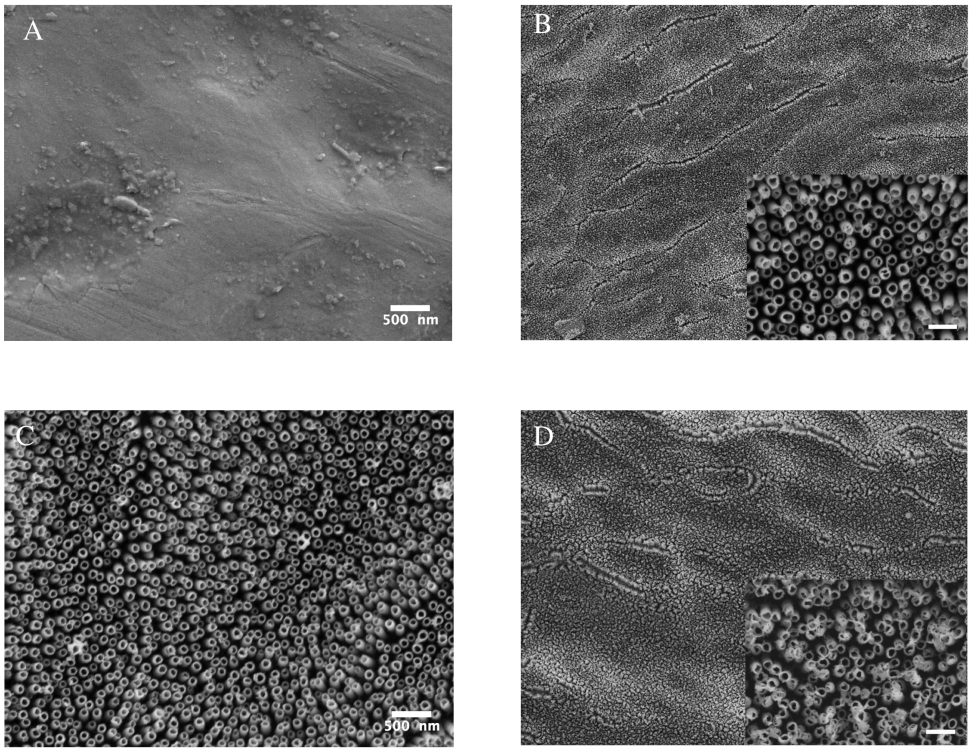

Figure 3. SEM images of the flat control Nitinol (A) and the upright nanotubular coating that was synthesized on top of superelastic Nitinol with outer nanotube diameters of approximately 110 nm (B), 90 nm (C) and 70 nm (D). Scale bars are 300 nm in B and C.

The nanotubular coating can be observed in the SEM images in Figure 3. As seen in Figure 3B, the nanotubes formed under such conditions have, on average, an outer diameter of about 110 nm. We were also able to produce nanotubes of about 90 nm in outer diameter by decreasing the anodization voltage to 70 V (Figure 3C). When I modified the electrolyte solution to contain 1.4 g NH_4F and anodized for 4 minutes at 85 V, I obtained nanotubes with an outer diameter of about 70 nm (Figure 3D). In contrast,

the control Nitinol substrate appears relatively free of topographical structures (Figure 3A).

2.2 Characterization of nanotubular coating

A

Element	Weight (%)	Atomic (%)	Compound (%)	Formula
Ti	32.14	20.62	53.62	TiO_2
Ni	36.45	19.07	46.38	NiO
O	31.41	60.31		
Total	100.00			

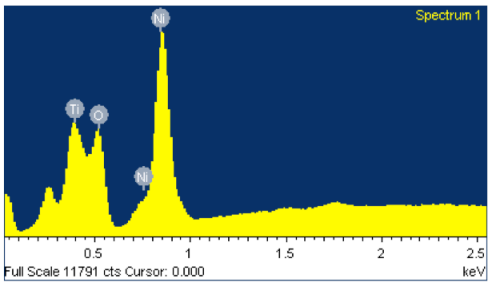

B

Element	Weight (%)	Atomic (%)	Compound (%)	Formula
Ti	41.11	46.11	-	-
Ni	58.89	53.89	-	-
Total	100.00			

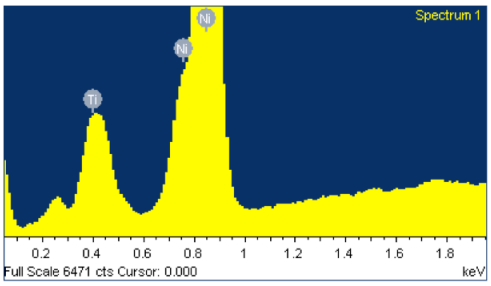

Figure 4. Energy dispersive X-ray spectroscopy (EDS) data of the nanotubular coated Nitinol (A) and the flat Nitinol control (B). Surface elemental analysis data is presented in the tables and EDS spectra. The nanotubular coating was found to consist of both NiO and TiO_2, while the control substrates had undetectable levels of a surface oxide layer.

We further characterized the nanotubular coating under an energy dispersive X-ray spectrometer (EDS). The EDS spectrum and elemental analysis of the region of the interest, as seen in Figure 4A, revealed the composition of the nanotubes to be a

combination of NiO and TiO_2. Figure 4B showed that the amount of oxide on the control Nitinol was too small to be detected by the EDS, thus corroborating the manufacturer's claim that the surface had been "pickled". However, Nitinol undergoes a natural process of passivation once in contact with air and we expect a thin, albeit undetectable through EDS, layer of oxide present on the control Nitinol substrates.

The biocompatibility of Nitinol relies to a large extent on the presence of an oxide layer to reduce the leaching of nickel ions[16]. Therefore, we conducted a nickel leaching experiment in which each 1 cm by 1 cm, nanotubes-coated and control Nitinol substrates were submerged in 1 mL of PBS solution in a standard 24-well tissue culture plate and placed in an incubator under standard tissue culture conditions. The 1 mL of PBS samples were retrieved at specific time points and replaced with fresh PBS solution. These PBS samples were then tested using the Nickel Assay Kit (Sigma-Aldrich) following the manufacturer's instructions (results in Figure 5). The nanotubes-coated Nitinol substrates have an average daily release rate of 37.6 ± 8.2 ng per substrate while the control Nitinol substrates have a mean daily release rate of 8.8 ± 5.0 ng per substrate. There was no statistically significant difference between the amount of nickel released (mean daily or cumulative) between the nanotubular coated and flat control Nitinol. The small amount of nickel released by the control Nitinol substrates proved the presence of an oxide layer formed as discussed above.

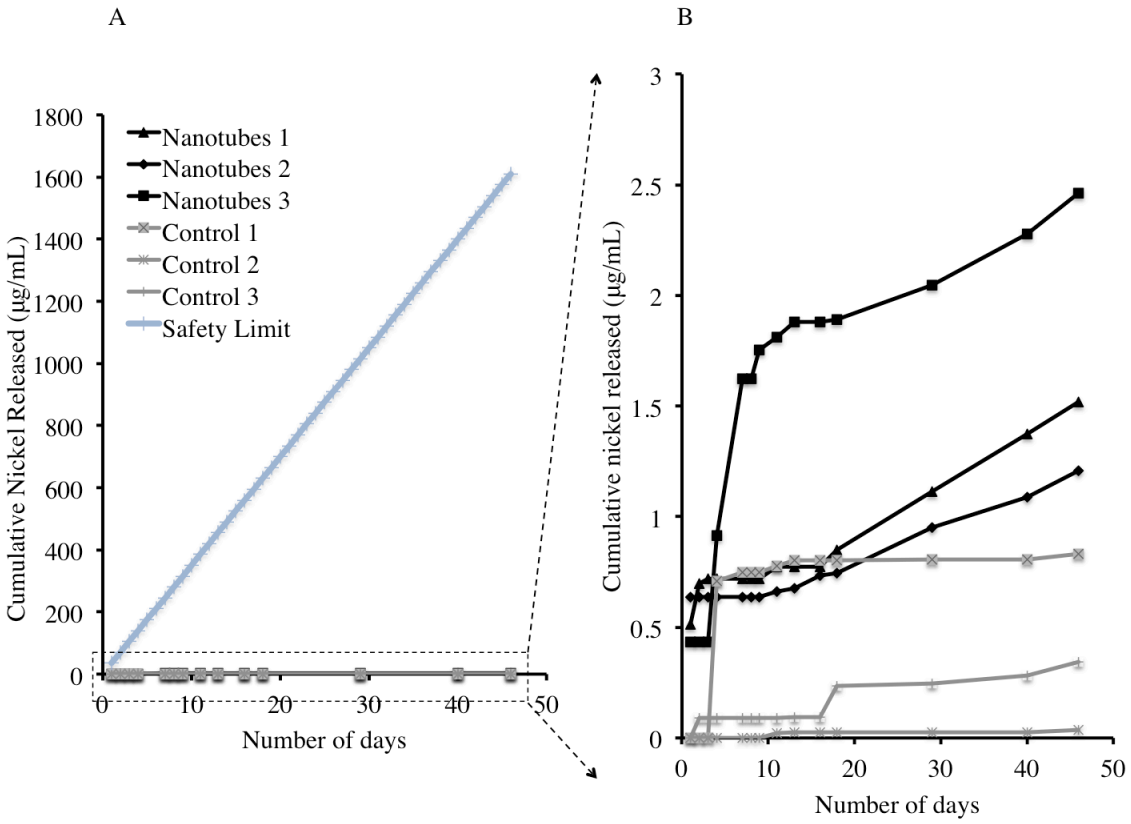

Figure 5. (A) Cumulative nickel released from nanotubular coated Nitinol (Nanotubes 1, 2 and 3) and flat control Nitinol (Control 1, 2 and 3) as compared to the intravenous nickel contamination limit (Safety Limit). (B) The same data enlarged, excluding the intravenous nickel contamination limit.

Although anodization increased the oxide layer on the Nitinol substrates, the process of nanotubes synthesis was, in essence, a generation of defects within the increased oxide layer, and could be a reason for the difference in the nickel release from the nanotubes-coated Nitinol substrates. Furthermore, the EDS surface elemental analysis in Figure 4A showed a similar atomic percentage of nickel and titanium on the nanotubular-coated substrates. Therefore, it was within expectations that there would be

some nickel released. It is, however, vital to note that these release levels of nickel were well under the tolerable limit of nickel contamination *in vivo*. In fact, they were at least three orders of magnitude lower than the intravenous nickel contamination limit of 35 μg/day (for a 70 kg man)[18].

Chapter 3

Regulation of Primary Human Aortic Endothelial Cell Functions

Re-endothelialization is a key factor in the prevention of restenosis and thrombosis because the process of stent deployment causes denudation of the endothelial layer[13–15,19]. I investigated the "pro-healing" potential of our nanotubular Nitinol coating by quantifying the migration, cell spreading and proliferation of primary HAEC (Lonza, USA). Cells were maintained and cultured under manufacturer's instructions and all experiments were conducted with cells between passage number 3 and 7.

3.1 HAEC morphology, cell spreading and growth

To investigate the cell morphology of HAEC on the different substrate surfaces, 1cm by 1cm 110nm-nanotubes-coated and control Nitinol substrates were sterilized with ethanol and rinsed twice with sterile PBS in 24-well tissue culture plates (VWR, USA) under sterile conditions. HAEC were seeded at a cell density of 10000 cells/well and cultured under manufacturer's instructions. At days 1, 4 and 7, the Nitinol substrates were rinsed in sterile PBS and transferred into fresh 24-well plates. The cells were fixed with 3.7% paraformaldehyde and blocked using a solution of 2.5% Bovine Serum Albumin, 0.1% triton-X and PBS. They were then actin-stained using FITC-conjugated phalloidin and nuclei-stained using DAPI, following manufacturer's instructions (Millipore, USA). These samples were then imaged under a Nikon C1si spectral confocal microscope (Figure 6A and 6B). Using ImageJ, I quantified cell spreading (Figure 6C) on these substrates by measuring the average surface area per cell by the actin staining and

normalizing it to the control. The cell number was also determined with ImageJ and the results can be seen in Figure 6D.

I observed a morphological difference between the HAEC cultured on the nanotubular coated Nitinol and the flat controls (Figure 6A and 6B). HAEC cultured on the nanotubes-coated Nitinol appeared to be individually larger and more spread out than those cultured on the flat control. They also displayed a more elongated and extended morphology. Here, I have shown that by creating a nanotubular coating, I could increase the cell surface area of HAEC cultured on Nitinol by about two-fold (Figure 6C). This substantiates previous literature that showed that mechanical factors, chemical factors or surface topography can be utilized to control cell morphology[14,20,21]. As seen in Figure 6D, the number of HAEC on nanotubular coated Nitinol was similar over the course of 7 days in culture while the number of HAEC on the control was greater by days 4 and 7. This showed that proliferation of HAEC was not increased on the nanotubular coating.

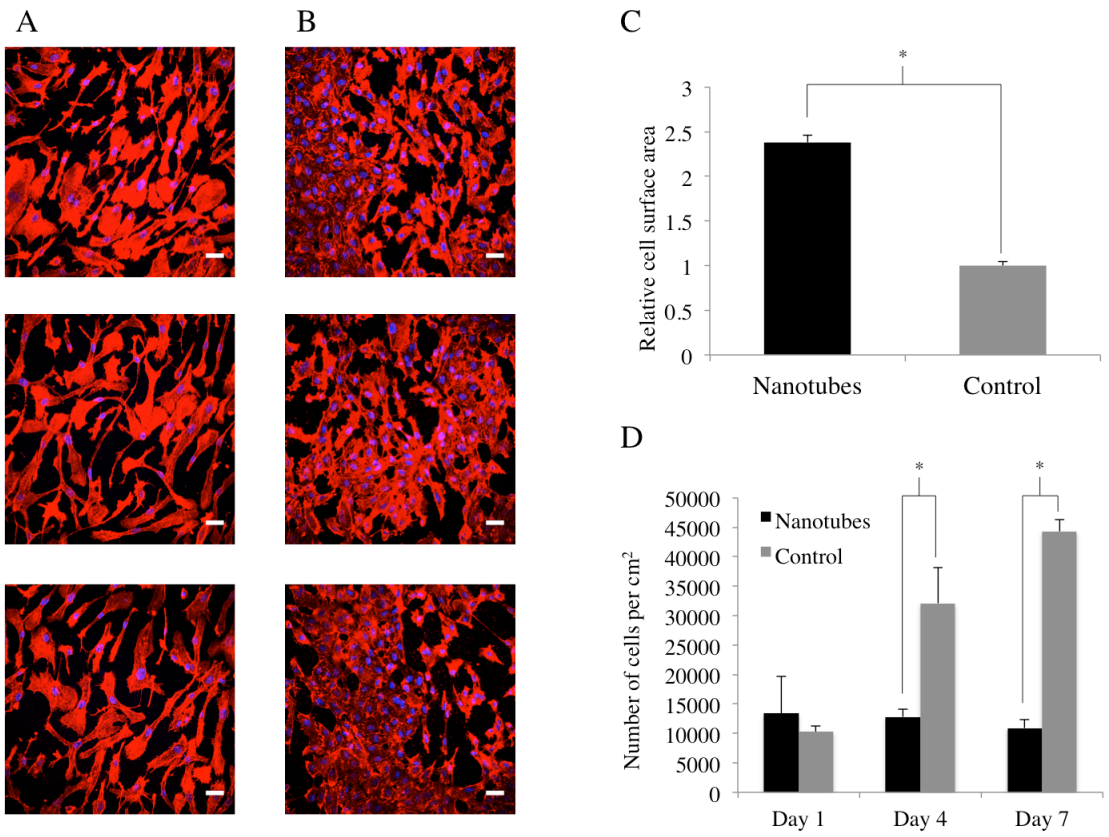

Figure 6. Fluorescence microscopy images of HAEC on nanotubular coated Nitinol (A) and flat control Nitinol (B) after 7 days of culture. FITC-phalloidin staining of F-actin is shown in red while DAPI staining of cell nuclei is shown in blue. Scale bars are 50 μm. Cell spreading is represented by the average cell surface area (C) normalized to that of the control, while HAEC growth (D) is represented in number of cells per cm^2 over a period of 7 days. * = $p < 0.01$, N = 5.

3.2 Effects of nanotube diameter on HAEC growth

Previous studies on TiO_2 nanotubes have shown that endothelial cells proliferated significantly faster on nanotubes with smaller diameters (15 nm as compared to 100 nm)[22]. Therefore, I set up an experiment with 110 nm and 70 nm nanotubes-coated

Nitinol substrates for investigating the growth of HAEC. As shown in Figure 7, there was no significant difference in HAEC number between 110 nm and 70 nm substrates for both 1 day and 7 days of culture. However, there remained a significant difference in HAEC number at day 7 of culture between the nanotubes-coated substrates and the flat control Nitinol. Therefore, I did not observe any significant effects on HAEC adhesion and proliferation when decreasing the nanotube diameters from 110 nm to 70 nm.

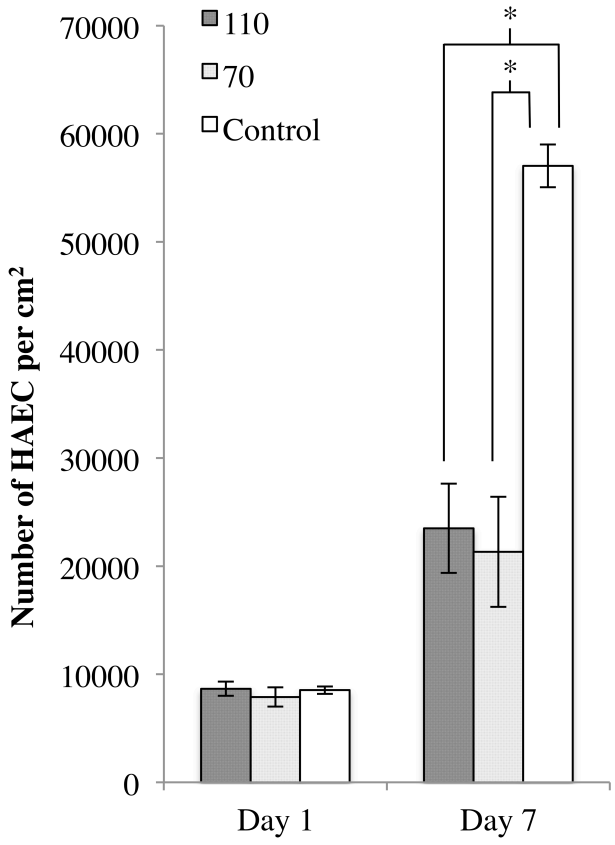

Figure 7. HAEC numbers are shown after 1 and 7 days of culture. There was no significant difference in the number of HAEC adhered after day 1. However, there was a significant difference in the number of HAEC on 110 and 70 as compared to Control after 7 days of culture. One-way ANOVA for day 7 ($F(2,6) = 25.648$, $p = 0.001$). N = 3, * = $p < 0.01$.

3.3 HAEC migration

As previously mentioned, the implantation of a stent typically results in the denudation of the endothelium at the lesion site. One of the most important factors for re-endothelialization is the migration of endothelial cells from the surrounding region into the lesion site. For purposes of studying the migration of HAEC in the context of stenting, a typical scratch assay is inappropriate. In the context of stenting, the endothelial cells have to migrate onto and across the struts of the stent from healthy neighboring endothelium. Therefore, I decided to perform the migration assay detailed by Sprague et al[23].

In this method, as depicted in Figure 8a, the deployment of a stent was simulated by "implantation" of the substrate of interest onto a confluent endothelial cell layer and then quantifying the number of cells that migrated onto the substrate. First, in a 12-well tissue culture plate, I seeded HAEC onto a rat tail collagen (Fisher, USA) gel with a concentration of 4mg/mL and cultured them to confluency. Then I carefully pushed the 1 cm by 1 cm nanotubes-coated Nitinol and control Nitinol substrates into the gels on top of the cells. The nanotubular coating was facing up in the setup. After 4 days of culture, we carefully removed the substrates, transferred them to fresh 24-well tissue culture plates and quantified the number of cells on each substrate using the CyQuant assay (Molecular Probes, USA) according to the manufacturer's instructions. As seen in Figure 8b, the number of HAEC on the nanotubular coated Nitinol substrates were significantly greater (t-test, $p < 0.001$) than that on the control Nitinol substrates. This increase in migration corresponds to that reported by several studies on nanotubular titania

surfaces[15,24,25]. Since migration is the key part to wound healing, a modification of the surface of the stent to increase the migration of HAEC onto the stent surface could prove vital in the healing of the endothelium. The recovery of the endothelium would also lead to the reduction in the migration of the HASMC into the intima and the proliferation of these cells[2,14], ultimately improving the overall viability of the vessel.

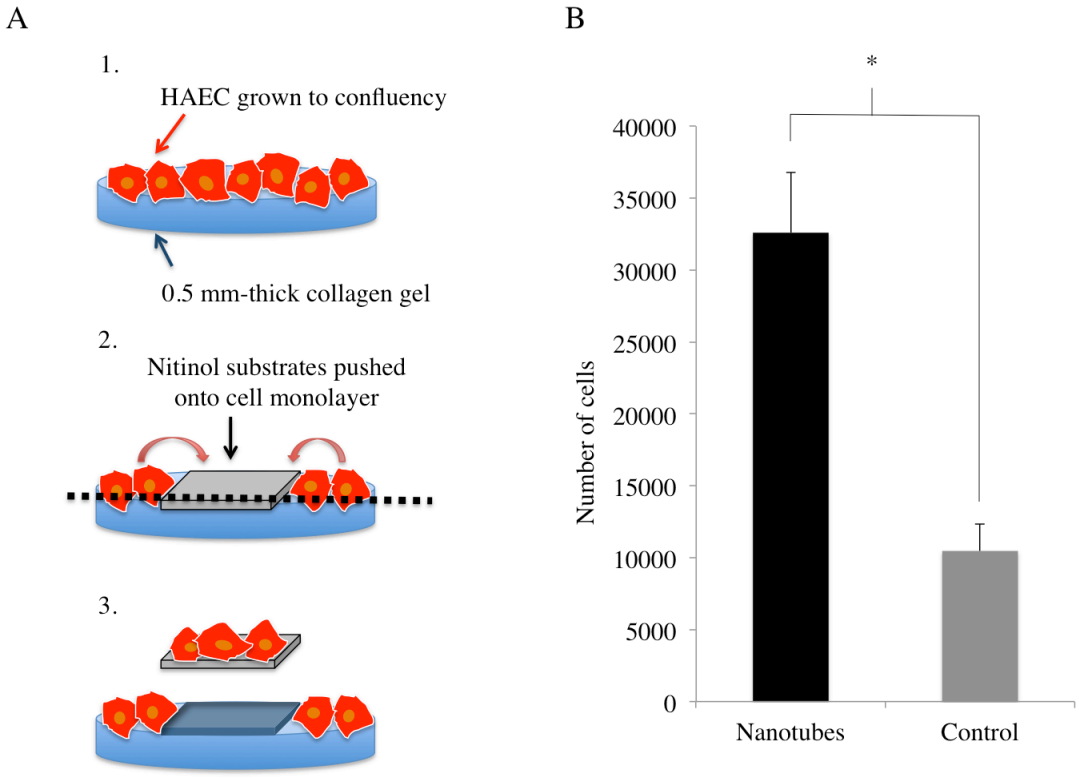

Figure 8. Nanotubular coated Nitinol increased the migration of HAEC. The schematic (A) describes the migration assay used while the data (B) shows a significant increase in migration of HAEC from the collagen gel onto the nanotubular coated Nitinol as compared to flat control Nitinol. * = $p < 0.001$, N = 5.

3.4 Effects of nanotube diameter on HAEC migration

After observing the significant increase, I proceeded to investigate the effects of nanotube diameter on HAEC migration. I repeated the experiment using Nitinol substrates with nanotube diameters of 110 nm, 70 nm and flat control. As shown in Figure 9, both 110 and 70 substrates demonstrated a similar increase in HAEC migration as compared to control. Therefore, changing the nanotube diameter from 110 nm to 70 nm did not significantly affect the migration of HAEC.

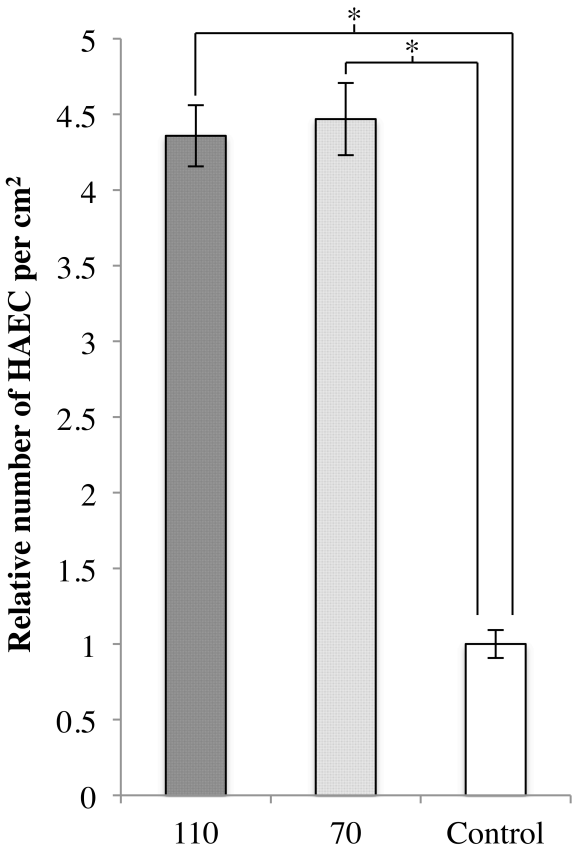

Figure 9. Relative number of HAEC that migrated onto each substrate after 4 days, normalized to Control. One-way ANOVA ($F(2,9) = 109.557$, $p < 0.001$). N = 4, * = $p < 0.00001$.

3.5 HAEC collagen production

The production of collagen is an important factor to consider for re-endothelialization. In particular, type IV collagen is a major component of the basement membrane[26]. The formation of the basement membrane allows the endothelium to heal and presents a physical barrier that separates the vascular smooth muscle cells in the media layer from the intima[26]. Another study has shown that fibrillar collagen decreases the proliferation of vascular smooth muscle cells through the $\alpha 2\beta 1$ signaling pathway[27]. In the context of preventing restenosis, the increase in the production of collagen by HAEC either as soluble factors or for the formation of ECM has the potential to reduce the migration and proliferation of HASMC.

HAEC were seeded onto the Nitinol substrates and cultured in 24-well tissue culture plastic for 7 days using the same protocols as aforementioned. On day 5, 1 mL of fresh media was replenished per well. This media was then collected on day 7 and the soluble collagen content was analyzed using the Sircol Collagen Assay (Bicolor, U.K.) following manufacturer's instructions (Isolation & Concentration protocol). Each Nitinol substrate was subsequently transferred to fresh 24-well tissue culture plastic and gently rinsed with sterile PBS. ECM collagen extraction was carried out following manufacturer's instructions with ice-cold 0.5 M acetic acid (Sigma-Aldrich) and 0.1 mg/mL pepsin (Sigma-Aldrich) solution. Collagen content was normalized per cell and to the control group, using average cell numbers obtained from the cell growth assays.

As seen in Figure 10A and B, there is a significant increase in the production of collagen for HAEC cultured on 110 and 70 as compared to Control. There was also a significant difference between the collagen released into the media between HAEC cultured on 110 and 70. For endothelium healing, collagen production by endothelial

cells is required to form the ECM upon which they grow. The increase in HAEC collagen production may suggest the potential of our coatings to provide a 'pro-healing' surface for the recovery of denuded endothelium and consequently, due to the previously mentioned reasons, aid in the prevention of restenosis.

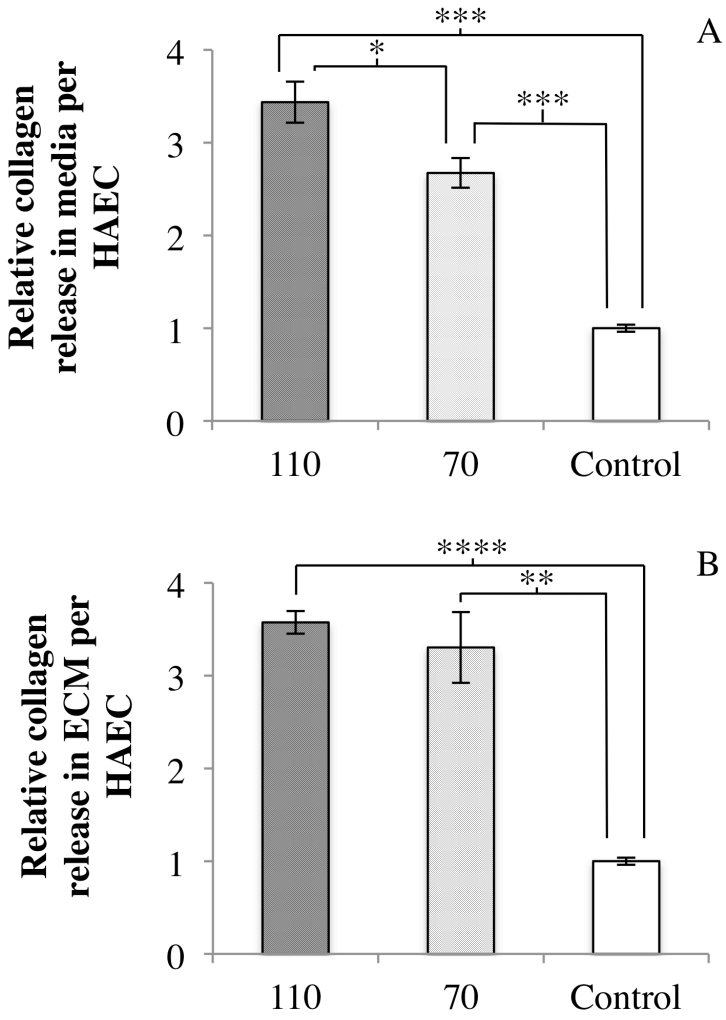

Figure 10. Relative collagen production per HAEC normalized to Control. A) Collagen released into media between Days 5 and 7 of HAEC culture. One-way ANOVA ($F(2,11) = 48.885$, $p < 0.001$). N = 5. B) Collagen laid down in ECM at the end of 7 days of HAEC culture. One-way ANOVA ($F(2,6) = 36.943$, $p < 0.001$). N = 3. * = $p < 0.05$, ** = $p < 0.01$, *** = $p < 0.001$, *** = $p < 0.0001$.

3.6 HAEC elastin production

Another protein of interest for the modulation of restenosis is elastin. Elastin plays significant roles in arterial morphogenesis, homeostasis, structural support and regulation of vascular smooth muscle cell function[28–30]. A previous study has shown that delivering exogenous elastin *in vivo* to porcine vessels that were injured reduced NIH[28].

HAEC were seeded onto the Nitinol substrates and cultured in 24-well tissue culture plastic for 7 days using the same protocols as mentioned above. On day 7, each Nitinol substrate was carefully transferred into fresh 24-well tissue culture plastic and gently rinsed in sterile PBS. The Fastin Elastin Assay (Bicolor, U.K.) was used to quantify the α-elastin content (soluble tropoelastins, lathyrogenic elastins and insoluble elastins) from the cells following manufacturer's instructions. Elastin production was normalized by cell number and to Control.

In Figure 11, there is a significant difference in the elastin production of HAEC cultured on 110, 70 and Control. HAEC on 70 demonstrated an increase of more than 4 times the amount of elastin produced as compared to control, while 110 showed an even greater increase of more than 7 times. This trend of increasing elastin production as nanotube diameter increases is similar to that seen in Figure 10A for soluble collagen production in HAEC.

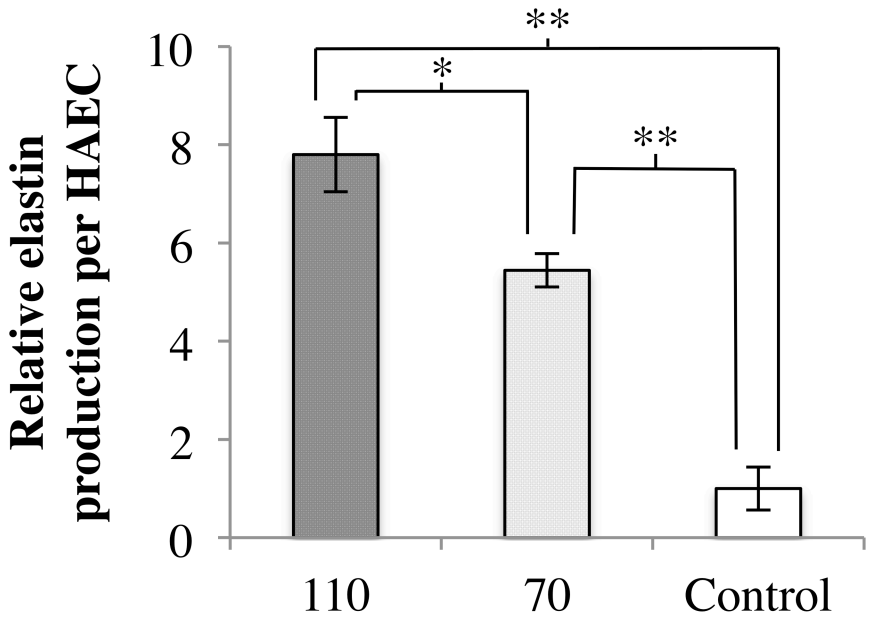

Figure 11. Relative elastin production per HAEC normalized to Control. Elastin production was significantly different between 110, 70 and Control. One-way ANOVA ($F(2,6) = 40.470$, $p < 0.001$). N = 3, * = $p < 0.05$, ** = $p < 0.01$.

Chapter 4

Regulation of Primary Human Aortic Smooth Muscle Cell Functions

In the process of restenosis, HASMC respond to the injury of the vessel caused by percutaneous coronary intervention. They migrate through the vessel walls, begin proliferating excessively and release ECM proteins such as collagen[2], resulting in restenosis. I wanted to investigate the effects of the nanotubular Nitinol coatings on primary HASMC (Lonza, USA) between passage number 3 and 7.

4.1 HASMC morphology, alignment and growth

I studied the effect of the nanotubular Nitinol coating on HASMC proliferation by the same methods as previously mentioned for HAEC proliferation. The nanotubes-coated Nitinol and control Nitinol were similarly prepared and the HASMC were seeded at a density of 10000 cells/well in 24-well tissue culture plates. At days 1, 4 and 7, the substrates were rinsed with PBS, transferred to fresh 24-well tissue culture plates, and actin- and nuclei-stained with DAPI and FITC-Phalloidin respectively. The cells were imaged and counted in ImageJ, and the results are shown in Figure 12C.

By day 7, I observed a significant difference (t-test, $p < 0.01$) in HASMC numbers between nanotubes-coated Nitinol and control Nitinol substrates. Furthermore, by day 7, the cells on control Nitinol have begun to reach confluency, as seen in the images in Figure 12B. In the confluent cell clusters, the HASMC also began to exhibit alignment on the control Nitinol surfaces. In contrast, the HASMC on nanotubes-coated Nitinol (Figure 12A) were less confluent and not as aligned. In a stent scenario, we may

anticipate that the HASMC that have migrated to the lumen and come into contact with the nanotubular coating will exhibit less proliferation. Since vascular smooth muscle cell proliferation is observed in neointimal hyperplasia[2,3], this nanotubular coating strategy can be particularly useful in Nitinol stents.

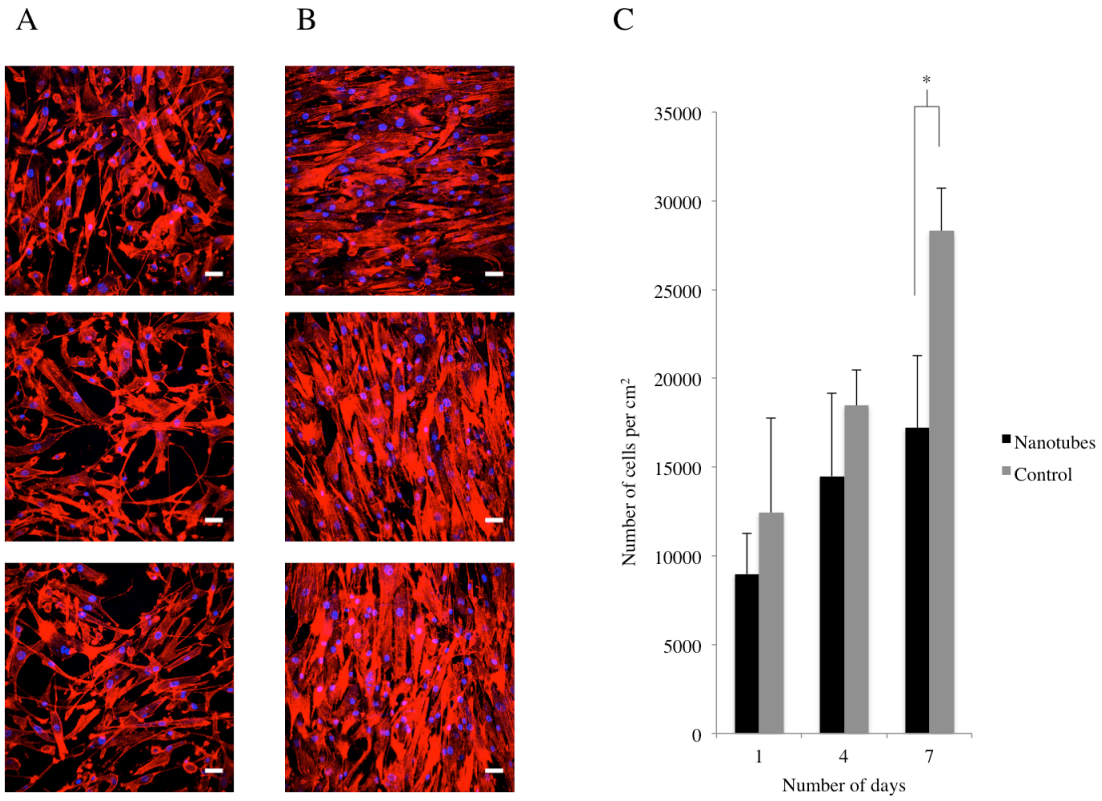

Figure 12. Fluorescence microscopy images of HASMC on nanotubular coated Nitinol (A) and flat control Nitinol (B) after 7 days of culture. FITC-Phalloidin staining of F-actin is shown in red while DAPI staining of cell nuclei is shown in blue. Scale bars are 50 μm. HASMC growth (C) is represented in number of cells per cm^2 over a period of 7 days. * = $p < 0.01$, N = 5.

4.2 Effects of nanotube diameter on HASMC growth

I set up an experiment with 110nm and 70nm nanotubes-coated Nitinol substrates for investigating the growth of HASMC. As seen in Figure 13, the number of HASMC that adhered to 110 was significantly lower than that on Control after 1 day in culture. Furthermore, the number of HASMC on both 110 and 70 were significantly less than that on Control at day 7. This suggests that both nanotubular coatings have the potential to reduce the adhesion and proliferation of HASMC in the context of restenosis. However, there was no significant difference between 110 and 70. This might suggest that, for the cellular functions of adhesion and proliferation, the HASMC respond similarly within the range of these size scales (110 and 70 nm) on Nitinol substrates. This phenomenon was also observed in previous studies with other cell types on titania nanotubes with diameters of these dimensions[22,31].

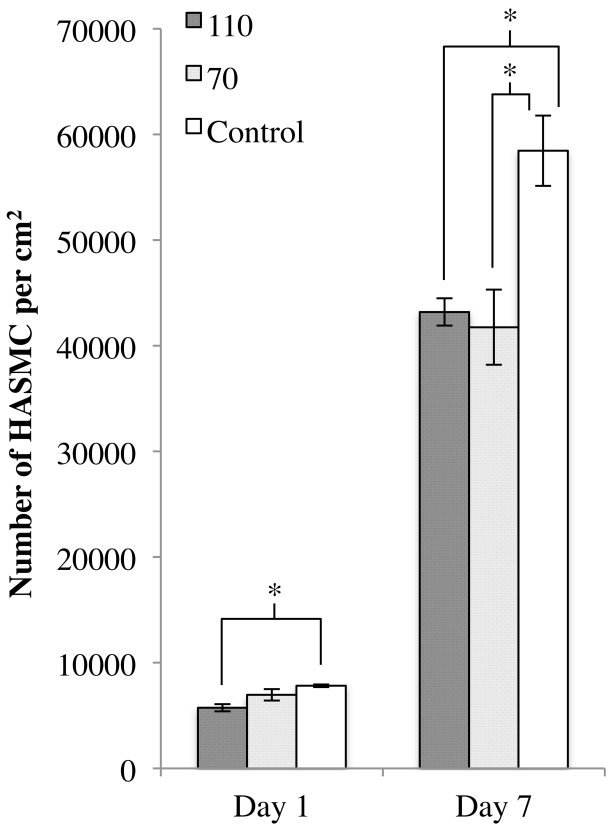

Figure 13. HASMC numbers are shown after culture for 1 and 7 days. At day 1, there was a significant difference in the number of HASMC that were adhered to the 110 as compared to Control. By day 7, there was a significant difference in the number of HASMC on 110 and 70 as compared to Control. One-way ANOVA for Day 1 ($F(2,12) = 7.719$, $p = 0.007$). One-way ANOVA for Day 7 ($F(2,12) = 10.121$, $p = 0.003$). N = 5, * = $p < 0.01$.

4.3 HASMC mRNA expression of Col1, Col3 and MMP2

Another major component of restenosis is the release of ECM proteins by the activated HASMC at the lesion site. I investigated the protein expression of collagen I in HASMC using immunofluorescent staining. The HASMC were seeded on 1 cm by 1 cm

nanotubes-coated and control Nitinol substrates I 24-well tissue culture plates at a seeding density of 30000 cells/well. After 48 hours, the cells were fixed and blocked as mentioned previously. They were then stained with mouse anti-collagen I primary antibody (Abcam) and Alexa Fluor 488 goat anti-mouse secondary antibody (Molecular Probes). Images were taken with the Nikon C1si spectral confocal microscope at the same laser intensity and processed with the same color balance (Figure 7A and 7B). Using quantitative PCR, I investigated the effects of the nanotubular Nitinol coating on the relative mRNA expression levels of the two major ECM proteins – collagen I and collagen III. I also looked at the relative mRNA expression levels of matrix metalloproteinase 2, which has been shown to be related to the migration of HASMC[26]. For this experiment, HASMC were seeded on 1cm by 1cm nanotubes-coated and control Nitinol substrates in 24-well tissue culture plates at a seeding density of 30000 cells/well. After 48 hours, the substrates were transferred into fresh 24-well tissue culture plates and 0.5% EDTA was used to life the cells from each substrate. After 6 minutes of exposure to EDTA, the cell suspension was transferred to an Eppendorf tube and centrifuged before aspirating the solution. mRNA isolation was performed on the cells using the Qiagen RNeasy Mini Kit (Qiagen, USA) and TRIzol Reagent (Ambion) following manufacturer's instructions. mRNA concentration and purity were determined using the Nano Drop ND-1000 Spectrophotometer (Thermo Scientific, USA). iScript cDNA Synthesis Kit (Bio-Rad, USA) was used to synthesize cDNA. Then, forward and reverse primers and Fast SYBR Green Master Mix (Applied Biosystems, USA) were used to amplify the cDNA of interest in an Applied Biosystems Viia7 real-time polymerase chain reaction system. Biological triplicates were performed for each substrate and the results

are presented as fold changes relative to the control using delta-delta CT values. A housekeeping gene, GAPDH, was used as the reference gene.

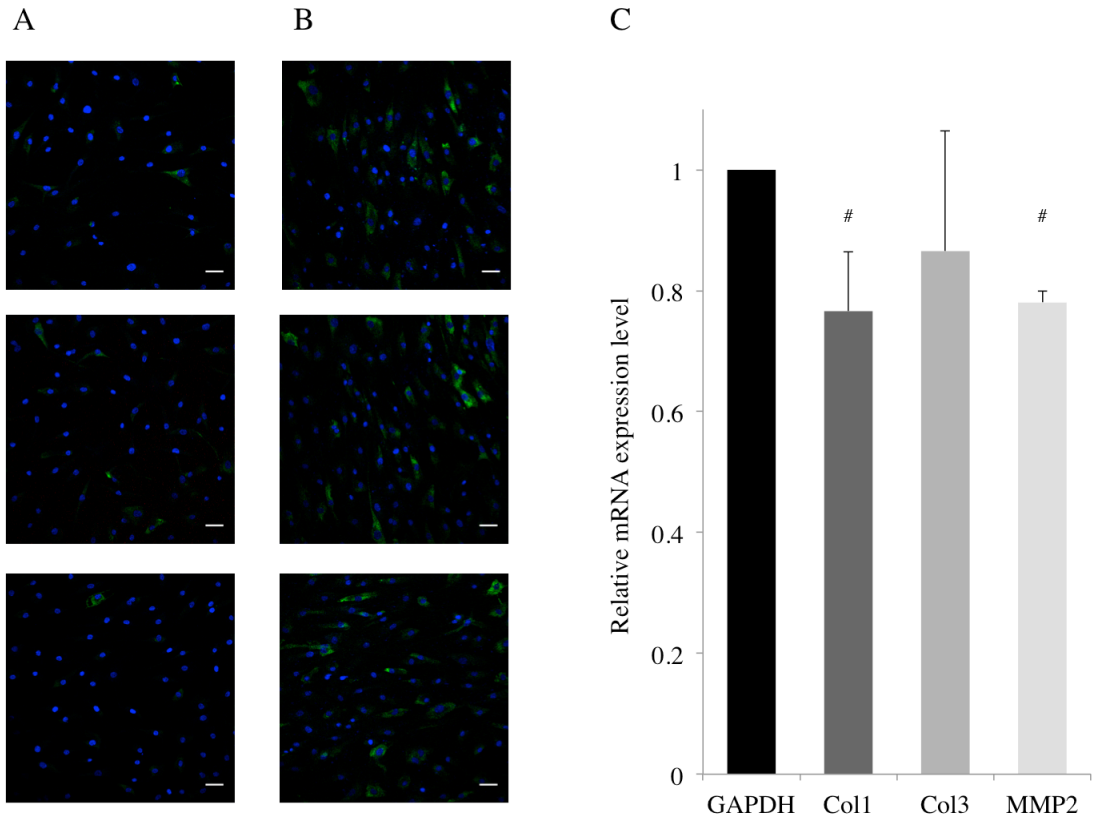

Figure 14. Immunofluorescent staining of Col1A (green) and DAPI staining of nuclei (blue) in HASMC grown on nanotubes-coated Nitinol (A) and the control (B). Relative mRNA expression levels of Collagen 1 (Col1), Collagen 3 (Col3) and Matrix Metalloproteinase 2 (MMP2) genes in HASMC (C) is presented as fold change using delta-delta CT values with GAPDH as the reference gene. # = $p < 0.05$, N = 5.

In Figure 14A, the immunofluorescent staining of Col1A (green) showed a lower protein expression in HASMC cultured on 110 nm nanotubes-coated Nitinol as compared

to those grown on the control (Figure 14B). The staining in the control group was less extensive and lower in intensity. This implied that fewer cells expressed detectable levels of the protein and among the cells that did, most of the individual levels of expression were lower. Furthermore, in Figure 14C, relative to GAPDH, the mRNA expression levels of collagen I was significantly downregulated on nanotubes-coated Nitinol as compared to control Nitinol. Collagen expression is an important factor because collagen is a major component of the neointima[2,32]. In the scenario of stent deployment, a nanotubular coating could reduce restenosis by directly affecting the formation of the neointima by downregulating the mRNA expression levels of collagen I in HASMC that are in contact with the surface. Furthermore, the downregulation of the mRNA expression of MMP2 is equally important in this scenario. HASMC are known to produce MMP2 to degrade the vessel basement membrane in order to migrate into the intima[33]. Thus, the downregulation in the mRNA expression levels of MMP2 in HASMC might be a sign of the reduction in the migration rates of the HASMC on the surface. If the HASMC in contact with the coated stent surfaces secrete less MMP2, our surface could potentially contribute in the reduction of the migration of other HASMC traveling into the intima.

4.4 HASMC collagen production

Based on the results from qPCR, I wanted to investigate the effects of 110nm and 70nm nanotubes-coated Nitinol substrates on the quantitative production of overall collagen in HASMC. As mentioned previously, for HASMC, the production of collagen is commonly associated with NIH and restenosis[2,19]. The effect of our coating on HASMC collagen production is much more attenuated than that on HAEC. In fact, one-way ANOVA did not reveal a significant difference among 110, 70 and Control (Figure

15A and B). While excessive proliferation and collagen production are typical characteristics of vascular smooth muscle cells with a 'synthetic' phenotype, the results from our cell growth assay and collagen assay suggest that HASMC cultured on our coatings may not adopt this phenotype.

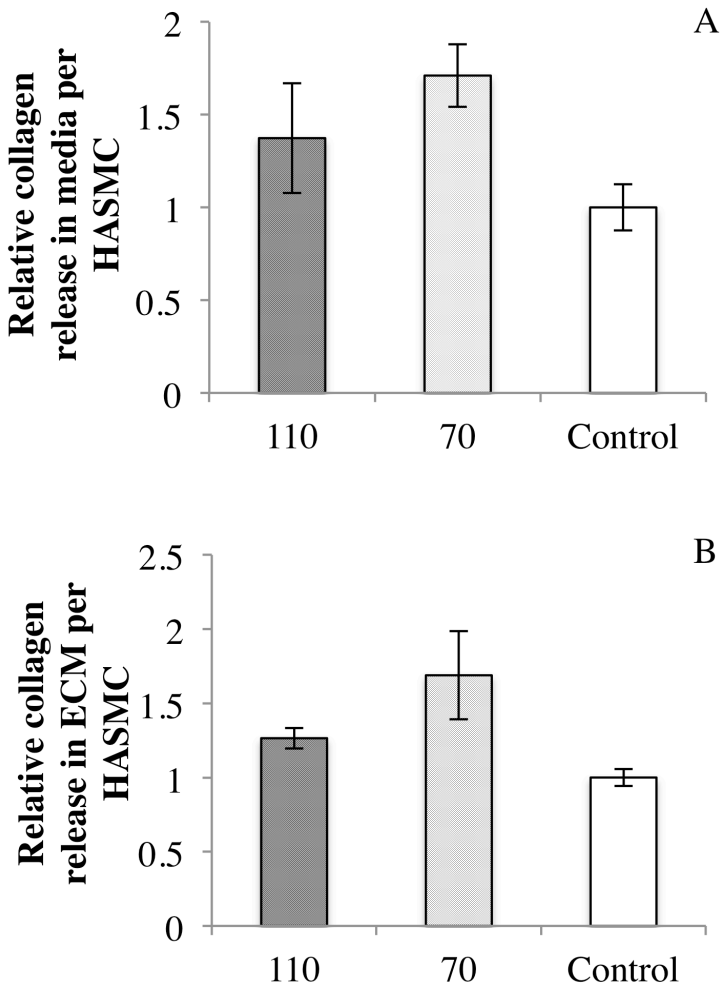

Figure 15. Relative collagen production per HASMC normalized to Control. A) Collagen released into media between Days 5 and 7 of HASMC culture. N = 5 B) Collagen laid down in ECM at the end of 7 days of HASMC culture. N = 3.

4.5 HASMC elastin production

As mentioned previously, elastin production is an important factor to consider in the prevention of restenosis. HASMC are the main producers of elastin in arteries; elastin is the most abundant ECM in the arteries and, beyond its role in maintaining structure, is essential for the proper development and maintenance of arteries[28–30]. Previously, I mentioned the therapeutic potential of elastin in preventing restenosis. To investigate the effect of 110 nm and 70 nm nanotubes-coated Nitinol substrates on HASMC elastin production, HASMC were seeded onto the Nitinol substrates and cultured in 24-well tissue culture plastic for 7 days using the same protocols as mentioned above. On day 7, each Nitinol substrate was carefully transferred into fresh 24-well tissue culture plastic and gently rinsed in sterile PBS. The Fastin Elastin Assay (Bicolor, U.K.) was used to quantify the α-elastin content (soluble tropoelastins, lathyrogenic elastins and insoluble elastins) from the cells following manufacturer's instructions. Elastin production was normalized by cell number and to Control.

In Figure 16, while ANOVA did not reveal statistical significance, we observed more than twice the amount the elastin produced in HASMC on 110 and 70 as compared to Control. The increase in elastin production of HASMC on our coatings may contribute towards the reduction of NIH by regulating HASMC proliferation and migration, and guide them away from the 'synthetic' phenotype.

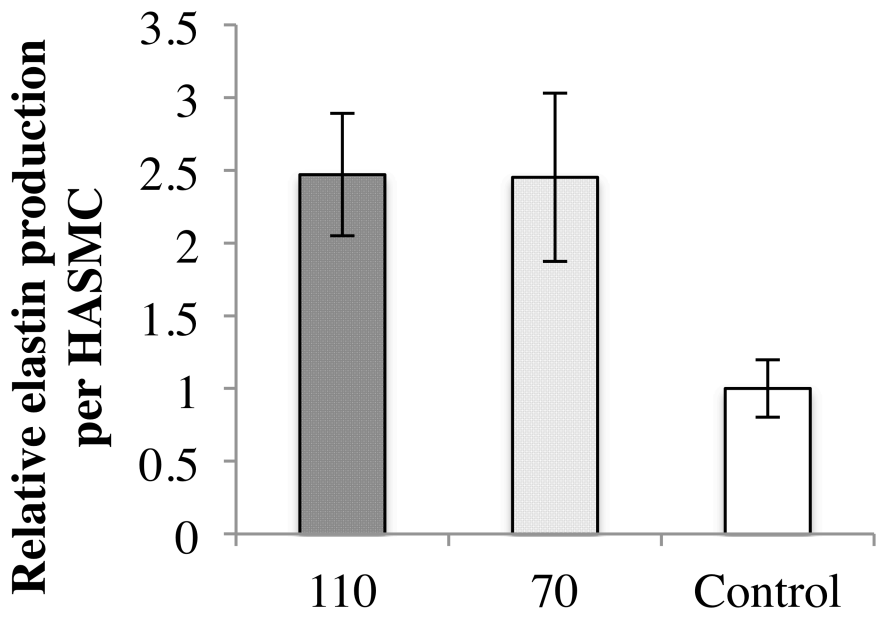

Figure 16. Relative elastin production per HASMC normalized to Control. N = 3.

4.6 Functional activation of HASMC

I wanted to characterize the functional activation of HASMC on the 110nm nanotubes-coated Nitinol substrates. Intercellular adhesion molecule-1 (ICAM-1) has been known to play an important role in the inflammatory response of vascular cells[34–37]. In HASMC, ICAM-1 induction in response to tumor necrosis factor-alpha (TNF-alpha) stimulation is a known inflammatory response that can be monitored by flow cytometery[37]. I seeded HASMC on nanotubes-coated and control Nitinol substrates for one day and identified the endogenous and TNF-alpha induced levels of ICAM-1 expression on the cell-surface using a FACSCalibur II Flow Cytometer operated by FACSQuest Software. To lift the cells prior to sorting, four technical replicates of the nanotubular or control surfaces were rinsed with PBS (Calcium and Magnesium free) with 0.04% EDTA and then incubated with PBS (Calcium and Magnesium free) with

0.04% EDTA at 37 ˚C until the cells had a round morphology, with a few already detached from the substrate. The PBS (Calcium and Magnesium free) with 0.04% EDTA was then transferred to a collection tube and replaced with 0.2 ml of 0.05% trypsin for 30-60 seconds at 37 ˚C. The flask was tapped sharply to dislodge the remaining cells and the cells were collected in medium. Cells were counted and pelleted at 160 x g for 4 minutes. Pelleted cells were resuspended in 100ul of DMEM/F12 medium at a concentration of 10^7/mL and fluorescently tagged for ICAM-1 (BioLegend 353107, Clone HA58) for 30 minutes on ice, as specified by the manufacturer. Finally, labeled cells were washed twice with PBS to remove any unbound antibodies and resuspended in DMEM/F12.

As shown in Figure 17, both the nanotubular and flat Nitinol surfaces had similar levels of endogenous ICAM-1 on the cell surface (plots labeled 'No TNF'). Furthermore, with 2 ng/mL and 10 ng/mL of TNF-alpha, I noticed no measurable differences in ICAM-1 expression between HASMC on nanotubular or flat control surfaces. Taken together, these data suggest that the nanotubular Nitinol surfaces do not induce inflammation when compared to the flat control Nitinol surface.

A B

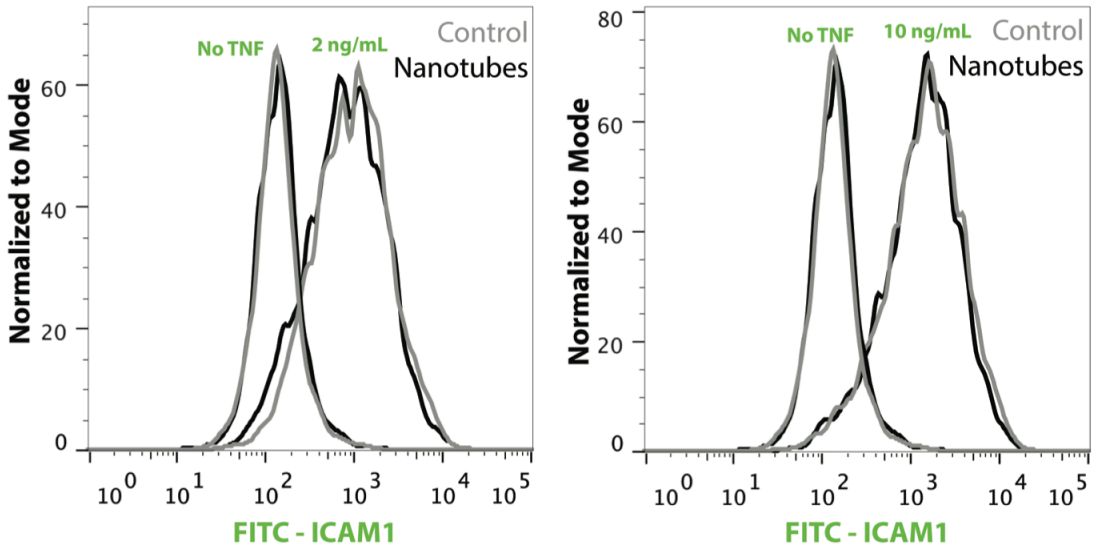

Figure 17. Flow cytometry histogram plots of HASMC stained for ICAM-1 and cultured on nanotubes-coated (Nanotubes) or flat control Nitinol (Control) surfaces. ICAM-1 induction with 2 ng/mL (A) and 10 ng/mL (B) of TNF-alpha is shown as a comparison to the endogenous level of the HASMC cultured on both surfaces (No TNF).

Chapter 5

Synthesis of Nanowell Coatings on Nitinol Stents

After investigating the effects of the Nitinol-based nanotubular coatings on HAEC and HASMC, I wanted to translate this coating onto a 3-dimensional complex structure – Nitinol stents.

5.1 Anodization conditions for synthesizing nanowell coatings on Nitinol stents

I discovered the anodization conditions for synthesizing a nanowell coating on Nitinol stents using the same iterative process I went through for the nanotubes coating. As shown in Figure 18, the Nitinol stent was held by a platinum wire on the anode of the anodization setup. The electrolyte solution consisted of 1.4 g of NH_4F, 490 mL of ethylene glycol and 7.5 mL of MQ water. Stents were cleaned via 3-step ultrasonication as detailed for Nitinol substrates.

Figure 18. Anodization setup for the synthesis of the nanowell coating on Nitinol stents.

To produce a homogenous layer of the coating, the length of time of anodization was different for Nitinol stents from different sources. For Nitinol stents purchased from Pulse Systems, the anodization was carried out for 3 minutes at 70 V to produce nanowell coatings as shown in Figure 19.

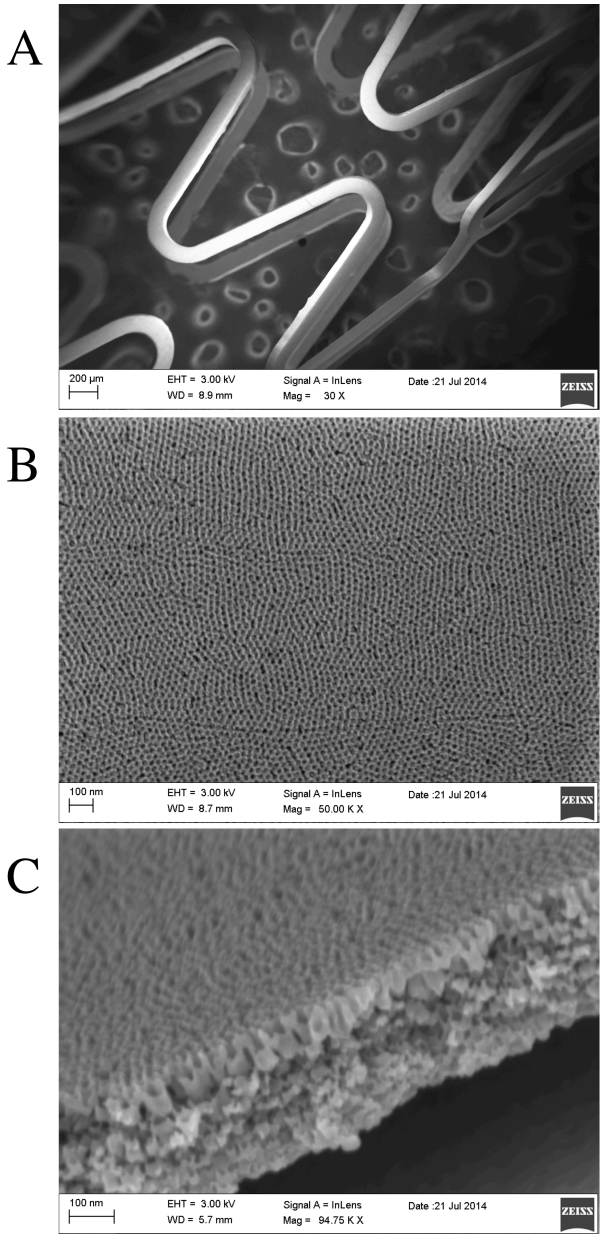

Figure 19. SEM images of the nanowell coating on a Nitinol stent from Pulse Systems. The coating covered the entire stent (A) and the nanowells were approximately 30 nm wide (B) and 30 nm tall (C).

To produce nanowell coatings on Nitinol stents purchased from Lumenous Device Technologies, the anodization was carried out for 5 min at 70 V. The nanowell coating is shown in Figure 20.

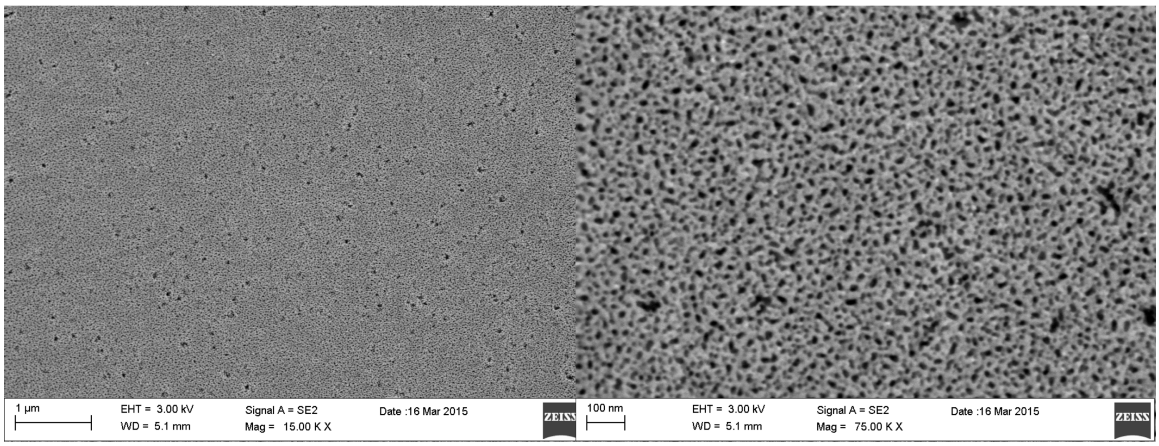

Figure 20. SEM images of nanowell coating on a Nitinol stent from Lumenous.

5.2 PLGA outer coating on nanowells-coated Nitinol stents

A nanowell coating on Nitinol stents may be the first step towards investigating the potential for such nanotopography to reduce restenosis in an *ex vivo* or *in vivo* setup. However, the nanowells also present a convenient depot for drug loading, thereby allowing a dual-action therapy of drugs and nanotopography. To pave the way for controlled or delayed release of drugs that may be loaded within the nanowell coating, I investigated the application of a poly(lactic-co-glycolic acid) (PLGA) (50:50) outer

coating on the nanowells-coated Nitinol stents. PLGA is FDA-approved and is in clinical use, while the 50:50 ratio formulation allows for a relatively faster degradation in the body via hydrolysis[38].

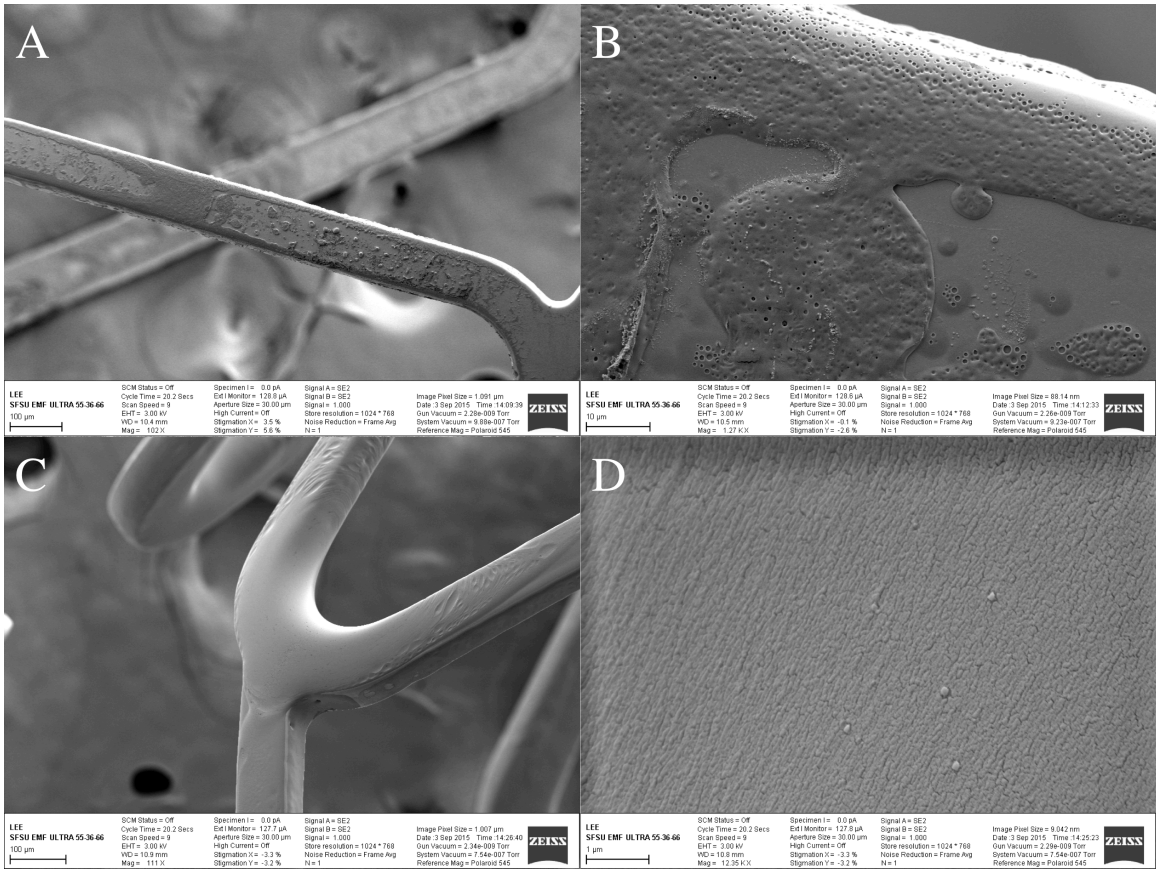

Figure 21. SEM images of Nitinol stents coated in PLGA (50:50) at a concentration of 10 mg/mL (A and B) and 100 mg/mL (C and D).

Nitinol stents were first anodized to produce the nanowell coating. Then, they were dip-coated into PLGA (50:50) dissolved in 2,2,2 – trifluoroethanol (TFE) at 10 mg/mL (Figure 21A and B) and 100 mg/mL (Figure 21C and D). As seen in Figure 21A and B, the concentration of PLGA (50:50) at 10 mg/mL was too low to create a coating that would envelop the entire surface area of the stent. However, when the concentration

was increased to 100 mg/mL, the amount of PLGA (50:50) was sufficient to form an even coating over the surface of the stent. If we were to load the nanowells with a drug, the thin coating of PLGA (50:50) could delay the initial burst of drug release and lead to a more controlled release. Furthermore, since PLGA (50:50) degrades relatively quickly in the body and the layer used to coat the stent is thin, the nanowells may be exposed and provide topographical cues for the regulation human vascular cells that are in contact with the surface. Moreover, it is possible to coat only one side (for example, the luminal side) of the stent, thereby allowing control over the nanotopographical cues and drug release from the stent.

5.3 Stability of PLGA (50:50) coating after crimping

To investigate the structural stability of the PLGA (50:50) coating, I crimped the PLGA-coated nanowell stent to 1.7 mm in diameter at room temperature. The stent was then released and self-expanded to its original diameter of 2.8 mm. Figure 22 shows that the PLGA coating remained stable with no signs of delamination. This stability was observed even at the troughs of the struts, which withstood the stresses during crimping.

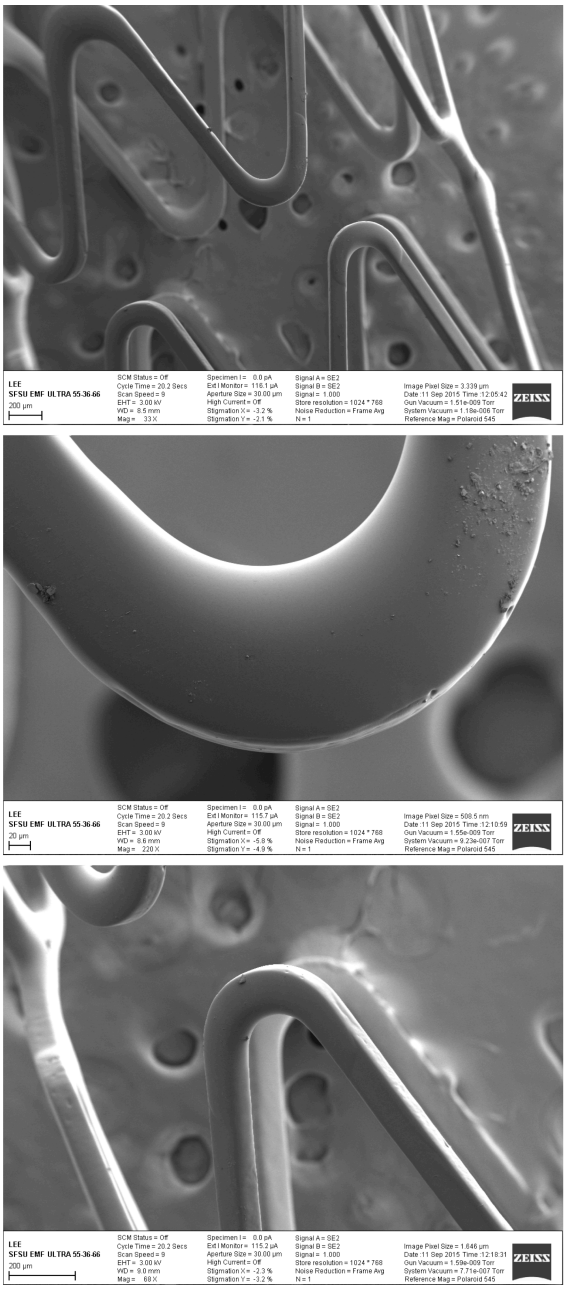

Figure 22. SEM images of PLGA (50:50) and nanowells-coated Nitinol stent after crimping to 1.7 mm in diameter and self-expansion.

Chapter 6

Concluding Remarks

Nanotubes-coated Nitinol presents an alternative approach towards reducing restenosis. The nanotubular coating provides a 'pro-healing' surface for HAEC, increasing their cell spreading, migration and collagen and elastin production. All these are vital for re-endothelialization. At the same time, HASMC demonstrate reduced adhesion, proliferation and mRNA expression of collagen I and MMP2. HASMC also showed increase elastin production on the nanotubes-coated Nitinol substrates. These findings show that the coating has the potential for reducing neointimal hyperplasia. Taken together, I've shown that the coating presents a balanced approach towards preventing restenosis.

I've also taken the project beyond the capacity of *in vitro* experiments by creating a nanowell coating on industrially manufactured Nitinol stents. With the studies on an outer layer of PLGA (50:50) coating, I've added an extra dimension of control over the potential for drug loading and release. Therefore, it is with great optimism that I conclude my graduate work on this subject and I look eagerly towards future advancements in this area.

Bibliography

1. Roger, V. L. *et al*. Heart disease and stroke statistics--2012 update: a report from the American Heart Association. *Circulation* **125,** e2–e220 (2012).
2. Rajagopal, V. Coronary restenosis: a review of mechanisms and management. *Am. J. Med*. **115,** 547–553 (2003).
3. Lüscher, T. F. *et al*. Drug-eluting stent and coronary thrombosis: biological mechanisms and clinical implications. *Circulation* **115,** 1051–8 (2007).
4. Khan, W., Farah, S. & Domb, A. J. Drug eluting stents: Developments and current status. *J. Control. Release* (2012). doi:10.1016/j.jconrel.2012.02.010
5. Mani, G., Feldman, M. D., Patel, D. & Agrawal, C. M. Coronary stents: a materials perspective. *Biomaterials* **28,** 1689–710 (2007).
6. Regan, C. P., Adam, P. J., Madsen, C. S. & Owens, G. K. Molecular mechanisms of decreased smooth muscle differentiation marker expression after vascular injury. *J. Clin. Invest*. **106,** 1139–47 (2000).
7. Joner, M. *et al*. Pathology of Drug-Eluting Stents in Humans. *J. Am. Coll. Cardiol*. **48,** 193–202 (2006).
8. Finn, A. V *et al*. Vascular responses to drug eluting stents: importance of delayed healing. *Arterioscler. Thromb. Vasc. Biol*. **27,** 1500–10 (2007).
9. Daemen, J. *et al*. Early and late coronary stent thrombosis of sirolimus-eluting and paclitaxel-eluting stents in routine clinical practice: data from a large two-institutional cohort study. *Lancet* **369,** 667–78 (2007).
10. Wenaweser, P. *et al*. Incidence and correlates of drug-eluting stent thrombosis in routine clinical practice. 4-year results from a large 2-institutional cohort study. *J.*

Am. Coll. Cardiol. **52,** 1134–40 (2008).

11. McFadden, E. P. *et al.* Late thrombosis in drug-eluting coronary stents after discontinuation of antiplatelet therapy. *Lancet* **364,** 1519–21 (2004).
12. Steffel, J. *et al.* Rapamycin, but not FK-506, increases endothelial tissue factor expression: implications for drug-eluting stent design. *Circulation* **112,** 2002–11 (2005).
13. Steffel, J. & Tanner, F. C. Biological effects of drug-eluting stents in the coronary circulation. *Herz* **32,** 268–73 (2007).
14. Peng, L., Eltgroth, M. L., LaTempa, T. J., Grimes, C. A. & Desai, T. A. The effect of TiO_2 nanotubes on endothelial function and smooth muscle proliferation. *Biomaterials* **30,** 1268–72 (2009).
15. Peng, L. *et al.* Whole genome expression analysis reveals differential effects of TiO_2 nanotubes on vascular cells. *Nano Lett.* **10,** 143–8 (2010).
16. Duerig, T., Pelton, A. & Sto, D. An overview of nitinol medical applications. *Mater. Sci. Eng.* **275,** 149–160 (1999).
17. Kim, J.-H., Zhu, K., Yan, Y., Perkins, C. L. & Frank, A. J. Microstructure and pseudocapacitive properties of electrodes constructed of oriented NiO-TiO_2 nanotube arrays. *Nano Lett.* **10,** 4099–104 (2010).
18. Sunderman, F. J. Potential toxicity from nickel contamination of intravenous fluids. *Ann Clin Lab Sci* **13,** 1–4 (1983).
19. Chan, J. M. *et al.* In vivo prevention of arterial restenosis with paclitaxel-encapsulated targeted lipid-polymeric nanoparticles. *Proc. Natl. Acad. Sci. U. S. A.* **108,** 19347–52 (2011).

20. Ma, Z., He, W., Yong, T. & Ramakrishna, S. Grafting of Gelatin on Electrospun Poly(caprolactone) Nanofibers to Improve Endothelial Cell Spreading and Proliferation and to Control Cell Orientation. *Tissue Eng*. **11,** 1149–58 (2005).

21. Levesque, M. J. & Nerem, R. M. The elongation and orientation of cultured endothelial cells in response to shear stress. *J. Biomech. Eng*. **107,** 341–7 (1985).

22. Park, J., Bauer, S., Schmuki, P. & von der Mark, K. Narrow window in nanoscale dependent activation of endothelial cell growth and differentiation on TiO2 nanotube surfaces. *Nano Lett*. **9,** 3157–64 (2009).

23. Sprague, E. A., Luo, J. & Palmaz, J. C. Human aortic endothelial cell migration onto stent surfaces under static and flow conditions. *J. Vasc. Interv. Radiol*. **8,** 83–92 (1997).

24. Brammer, K., Oh, S. & Gallagher, J. Enhanced cellular mobility guided by TiO_2 nanotube surfaces. *Nano Lett*. **8,** 786–793 (2008).

25. Park, J., Bauer, S., von der Mark, K. & Schmuki, P. Nanosize and vitality: TiO_2 nanotube diameter directs cell fate. *Nano Lett*. **7,** 1686–91 (2007).

26. Pauly, R. R. *et al*. Migration of cultured vascular smooth muscle cells through a basement membrane barrier requires type IV collagenase activity and is inhibited by cellular differentiation. *Circ. Res*. **75,** 41–54 (1994).

27. Koyama, H., Raines, E. W., Bornfeldt, K. E., Roberts, J. M. & Ross, R. Fibrillar collagen inhibits arterial smooth muscle proliferation through regulation of Cdk2 inhibitors. *Cell* **87,** 1069–78 (1996).

28. Karnik, S. K. *et al*. A critical role for elastin signaling in vascular morphogenesis and disease. *Development* **130,** 411–423 (2003).

29. Li, D. Y. *et al*. Elastin is an essential determinant of arterial morphogenesis. *Nature* **393,** 276–280 (1998).

30. Brooke, B. S., Bayes-Genis, A. & Li, D. Y. New insights into elastin and vascular disease. *Trends Cardiovasc. Med*. **13,** 176–181 (2003).

31. Brammer, K. S. *et al*. Improved bone-forming functionality on diameter-controlled TiO(2) nanotube surface. *Acta Biomater*. **5,** 3215–23 (2009).

32. Nagler, A. *et al*. Inhibition of collagen synthesis, smooth muscle cell proliferation, and injury-induced intimal hyperplasia by Halofuginone. *Arterioscler. Thromb. Vasc. Biol*. **17,** 194–202 (1997).

33. Chen, J. *et al*. PDGF-D contributes to neointimal hyperplasia in rat model of vessel injury. *Biochem. Biophys. Res. Commun*. **329,** 976–83 (2005).

34. Braun, M., Pietsch, P., Felix, S. B. & Baumann, G. Modulation of Intercellular Adhesion Molecule-1 and Vascular Cell Adhesion Molecule-1 on Human Coronary Smooth Muscle Cells by Cytokines. **2579,** 2571–2579 (1995).

35. Braun, M., Pietsch, P., Schror, K., Baumann, G. & Felix, S. B. Cellular adhesion molecules on vascular smooth muscle cells. *Cardiovasc. Res*. **41,** 395–401 (1999).

36. Wright, P. S., Cooper, J. R., Kropp, K. E., Busch, S. J. & Elisa, C. Induction of Vascular Cell Adhesion Molecule-1 Expression by IL-4 in Human Aortic Smooth Muscle Cells Is Not Associated With Increased Nuclear NF- B Levels. **389,** 381–389 (1999).

37. Couffinhal, T. *et al*. Tumor necrosis factor-alpha stimulates ICAM-1 expression in human vascular smooth muscle cells. *Arterioscler. Thromb. Vasc. Biol*. **13,** 407–414 (1993).

38. Ramchandani, M., Pankaskie, M. & Robinson, D. The influence of manufacturing procedure on the degradation of poly(lactide-co-glycolide) 85:15 and 50:50 implants. *J. Control. Release* **43,** 161–173 (1997).

PUBLISHING AGREEMENT

It is the policy of the University to encourage the distribution of all theses, dissertations, and manuscripts. Copies of all UCSF theses, dissertations, and manuscripts will be routed to the library via the Graduate Division. The library will make all theses, dissertations, and manuscripts accessible to the public and will preserve these to the best of their abilities, in perpetuity.

I hereby grant permission to the Graduate Division of the University of California, San Francisco to release copies of my thesis, dissertation, or manuscript to the Campus Library to provide access and preservation, in whole or in part, in perpetuity.

Author Signature  _____ Date 17th December 2015